Research Article

Duaa Al-Jeznawi, Ismacahyadi Bagus Mohamed Jais*, Bushra S. Albusoda, and Norazlan Khalid

The slenderness ratio effect on the response of closed-end pipe piles in liquefied and non-liquefied soil layers under coupled static-seismic loading

https://doi.org/10.1515/jmbm-2022-0009
Received Feb 17, 2022; accepted Mar 09, 2022

Abstract: This study presents the findings of a 3D finite element modeling on the performance of a single pile under various slenderness ratios (25, 50, 75, 100). These percentages were assigned to cover the most commonly configuration used in such kind of piles. The effect of the soil condition (dry and saturated) on the pile response was also investigated. The pile was modeled as a linear elastic, the surrounded dry soil layers were simulated by adopting a modified Mohr-Coulomb model, and the saturated soil layers were simulated by the modified UBCSAND model. The soil-pile interaction was represented by interface elements with a reduction factor (R) of 0.6 in the loose sand layer and 0.7 in the dense sand layer. The study was compared with the findings of 1g shaking table tests which were performed with a slenderness ratio of 25. In the validation case, there was a clear correlation between the laboratory findings and the numerical analyses. It was observed that the failure mechanism is influenced by the soil condition and the slenderness ratio to some extent. Under the dry soil condition, no base pile deformation was observed; However, tip pile movement was observed under the saturated soil condition with pile slenderness ratios of 25 and 50. The findings of this study are also aimed to include an approximation of the long-term deformations at the ground surface which has experienced shaking.

Keywords: 3D finite element model, liquefaction, modified Mohr-Coulomb model, slenderness, UBCSAND model

1 Introduction

Pile foundation is usually subjected to vertical loads. However, in different circumstances, some piles are subjected to vertical loads, lateral loads, and moments. Traffic, seismic events, wind, and earth pressure are the elements that contribute to lateral forces to the pile. The irregularity of the axial loads, the fixity of the building to the ground, and the position of the resultant horizontal forces on the pile concerning the ground surface are all factors that might contribute to moments in the pile. When a horizontal load is imposed to the top of a pile that can move in a horizontal direction, the load is first absorbed by the ground surface. The ground surface, on the other hand, compresses elastically as well as some pressures are transferred to the soil at a deeper depth. Thus, the ground yields plastically as the lateral force is increased, and the applied load continues to deeper depths. There are cases where the length of the pile is insufficient for such a flexural stiffness to keep its significance (short pile). In this case, the passive resistance has reached its maximum at the pile head and tip, thus the whole pile rotates as a rigid body.

During such seismic events, the following are the main contributing loads to a pile; axial load due to inertial and kinematic influences, inertial load owning to the superstructure, and other loads related to kinematic effects (ground movement). Poulos and Davis [1, 2] stated that the resistance of the pile foundation in the horizontal direction is extremely critical in the construction of structures subjected to earthquakes, soil movement, and waves. Various studies have used the 3D finite element approach to evaluate the response of piles under lateral load [3–5].

Pile foundations may be classified into two types according to the ratio of the effective unsupported length (L) to the average pile diameter (D), such that when L/D>30 the

***Corresponding Author: Ismacahyadi Bagus Mohamed Jais:** School of Civil Engineering, College of Engineering, Universiti Teknologi MARA Shah Alam, 40450, Selangor, Malaysia; Email: ismac821@uitm.edu.my
Duaa Al-Jeznawi: School of Civil Engineering, College of Engineering, Universiti Teknologi MARA Shah Alam; Lecturer at College of Engineering, Al-Nahrain University, Baghdad, Iraq
Bushra S. Albusoda: University of Baghdad, College of Engineering, Iraq
Norazlan Khalid: School of Civil Engineering, College of Engineering, Universiti Teknologi MARA Shah Alam, 40450, Selangor, Malaysia

pile is considered as a long pile, and when L/D<20 the pile is considered as a short pile [6, 7]. Jie Han [8] stated that piles may classify as long, intermediate, and short piles based on their diameter and the critical length (T) such that D>=4T, 2T<D<4T, and D>=4T respectively. The critical length (T) is equal to $(E_p I_p/E_s)^{0.25}$, where E_p and E_s is the modulus of pile and soil respectively and I_p is the pile moment of inertia. Three possible failure modes are available when a pile is set with a pile cap that is prevented from rotating, short piles may move as a rigid body, whereas longer piles may first generate a plastic hinge at the pile cap zone, and then a plastic hinge further down the pile, as shown in Figure 1 [9]. Regardless of the fact that piles are designed with a high safety factor, some recent earthquakes have detected piles fail due to the creation of plastic hinges [9].

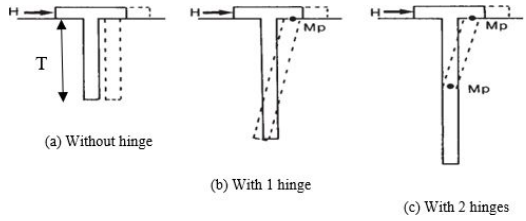

Figure 1: Pile failure modes due to lateral loads [9]

Bhattacharya and Tokimatsu [10] stated that the pile slenderness ratio is considered as the ratio of the effective length to the minimum radius of gyration. The authors supposed that the effective length is the pile length in liquefied soil layer and the minimum radius of gyration is the square root of the second moment of area divided by the pile cross-section area $\left(\sqrt{\frac{I}{A}}\right)$. The minimum radius of gyration of hollow pipe pile is equal to 0.35 times the pile outside diameter. Thus, the authors suggested that the pile is considered as a short column since the slenderness ratio is less than 50 [10]. The above were the main theories related to classifying the piles according to their slenderness ratio.

Bhattacharya and Bolton [11] stated that the majority of existing codes (Euro code 8 [12], NEHRP 2000 [13], and IS1893 [14]) ignore the factors that should be taken into account to prevent a pile from buckling owing to the axial force acting on it during soil liquefaction when confining pressure around the pile decreases. They mentioned that buckling is the most devastating type of failure, it appears rapidly, it needs a different design approach than bending, it depends on geometric stiffness and is almost independent of strength while bending is a stable mechanism that is based on strength. Iman *et al.* [15] experimentally studied the effect of slenderness ratio (from 12 to 30) on the laterally loaded pile (static load) embedded in loose and medium sand soil (RD=30% and 50%, respectively), their results showed that the slenderness ratio and the density of the surrounded soil are the essential parameters that affect the pile lateral resistance.

Since three-dimensional finite element analyses are nowadays commonly employed, this paper investigates the assessments of piles under combined static (50% of the allowable vertical load and 50% of the allowable lateral load) and dynamic load (Kope earthquake, PGA=0.82g) using this method. The results of the 3D finite element analysis of a single pile with different slenderness ratios and different soil conditions will be discussed in this paper.

2 Soil-pile model

Figure 2 shows the configuration of the soil-pile system considering different pile slenderness ratios. In this study, the slenderness ratio is taken as the ratio of unsupported pile length to the outside pile diameter (L/D). 3D finite element models were developed via MIDAS GTS NX software, considering the nonlinear characteristic of the intended model under the effect of combined static and dynamic loads. Modified Mohr-Coulomb (MMC) and modified UBCSAND[1] models were used for modeling the dry and saturated soil layers, respectively. The full details of the models' input parameters with the implemented boundary conditions and meshing were described by Al-Jeznawi *et al.* [16, 17]. For instance, young modulus was about 11 and 28 Mpa, friction

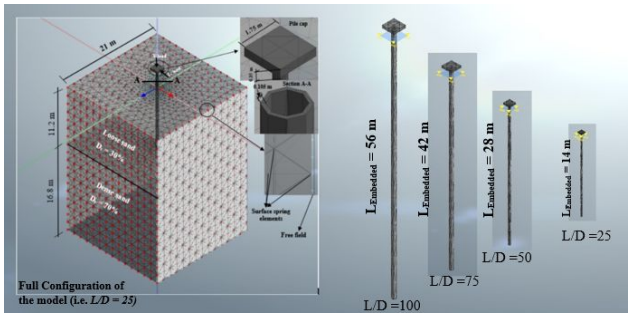

Figure 2: Configuration of soil-pile system with different pile slenderness ratios

1 UBCSAND model is a plasticity constitutive model of effective stress that can be used in complex stress deformation investigations of geotechnical engineering. This model was established particularly for sandlike soils with liquefaction potential during earthquake loading (e.g., sands and silty sands with a relative density less than about 80%).

angle was about 32° and 35°, poisons ratio was 0.3 for both loose and saturated layers, respectively. Soil unit weight was 13.5KN/m^3 and 16 KN/m^3 for dry loose and dense sand, respectively; and the effective unite weight was 9.11 KN/m^3 and 9.5 KN/m^3 for saturated loose and dense sand, respectively. The main input parameters for the saturated soil model were gathered through laboratory testing and then calibrated according to Beaty and Byrne [18].

Since the available 1g shaking table tests were all about the slenderness ratio of 25, which were performed by Hussein and Albusoda [19, 20], the current numerical models with L/D =25 are validated with these experimental findings. A full-scale model was numerically developed, 0.56 m as pile outside diameter and it was 0.105 m thick with 17.5 m length. The pile tip was located at 11.5 m above the soil bottom. The dimensions of the whole soil box were 21 m × 21 m × 28 m, the thickness of the loose sand layer was about 11.2 m and the dense sand layer was about 16.8 m. The pile was attached to an aluminum cover measuring 1.75 m × 1.75 m × 0.35 m in size. The above dimensions were maintained for the slenderness ratio of 25. However, with other slenderness ratios, the elements on the sides of the soil box were extruded to enlarge the box dimensions to be appropriate with the new slenderness ratio. Using 8 nodes tetrahedral components, a very thin meshing was adopted to represent the attitude of soil-pile interaction under various earthquake excitations. To conduct the existing system, nonlinear static, and nonlinear time history analyses with three construction phases were adopted: the first step is to calculate the model self-weight (Gravity loading), the second phase is to calculate coupled static forces (allowable pile vertical and lateral loads), and the third phase is to apply the dynamic load (Kobe ground acceleration). During the first and second phases, static constraints were used; however, for dynamic analysis, new elements were designed to construct the soil surface spring (using elastic boundary conditions) and free field features were developed in the direction of the earthquake.

Consequently, different slenderness ratios were investigated by keeping the distance between the pile tip to the bottom of the soil box do not exceed 4D, and the box dimensions were exceeded the least lateral bounds on the pile lateral response according to the elastic approach; such that distance = 17D [21].

3 Results and discussion

A 3D finite element model was developed in this study using MIDAS GTS NX software. The model created refers to the 1g shaking table tests performed by Hussein and Albosuda [19, 20]. The main model consisted of an Aluminum pipe pile embedded in two sand layers with different densities (loose sand with RD=30% and dense sand with RD = 75%), as shown in Figure 2. The geotechnical parameters of the simulation were correlated using physical data of the soils used in the shake table tests, and the correlation was maintained throughout the calibration process to meet the actual soil characteristics.

The maximum deformation of the pile shaft under combined static-dynamic loads with different slenderness ratios under the conditions of dry and saturated soil layers is shown in Figure 3. For the dry conditions, there is roughly no lateral deformation within the dense sand layer because of the soil densification which in turn restricts the relative displacement of the pile. On the other hand, the pile lateral deformation was significant in the loose sand layer. The shape and the trend of the deformation weree different depending on the pile slenderness ratio. For high slenderness ratios (75 and 100), the pile experienced significant buckling within the maximum bending moment zone, as shown in Figure 4. It is noticed that the pile shaft experienced lateral displacement near the pile tip under the saturated conditions with the slenderness ratios of 25 and 50, as shown in Figure 3(b).

Under the effect of coupled static-dynamic loads with saturated soil layers, the pile cap totally deformed with the four slenderness ratios (Figure 3b). Overall, the pile lateral displacements were considered high and not applicable in reality. This huge deflection occurred because the intensity of Kobe acceleration is extremely high (0.82g), thus the stiffness of the Aluminum material might not be enough to tolerate the above dynamic excitation. Therefore, new models were developed to check how the lateral displacement is affected by the pile stiffness (EI). The new models developed with the same soil and pile conditions, thus three slenderness ratios selected were 25, 50, and 75, then the pile diameter increased by about 1.8% to become equal to 1 m instead of 0.56 m (in the previous cases). The new models results showed that the pile lateral deflection has decreased significantly by more than 70% regardless the effect of soil condition (dry and saturated), as shown in Figure 4. According to the geotechnical design criteria in Malaysia, the pile under the effect of lateral load and bending loads perpendicular to axis of the pile, is not allowed to move laterally at a maximum of 12 mm. Thus, slenderness ratios of 50 and less are only recommended to use under similar soil and pile conditions; particularly, in areas exposed to high earthquake intensity.

Figure 5 presents the maximum bending moment along the pile length under combined static-dynamic loads with

different slenderness ratios at dry and saturated soil layers. Generally, the trend of the bending moment in all models was similar and the maximum values were noticed in the loose sand layer and at the zone of liquefaction in the saturated soil layer. The numerical analysis showed that the bending moment of the pile embedded in saturated soil layers experienced a higher bending moment than in dry soil layers.

It is important to note that the numerical models presented in this paper were conducted with undrained effective stress conditions. Thus, the values of excess pore water pressure ratios were determined with significant pile

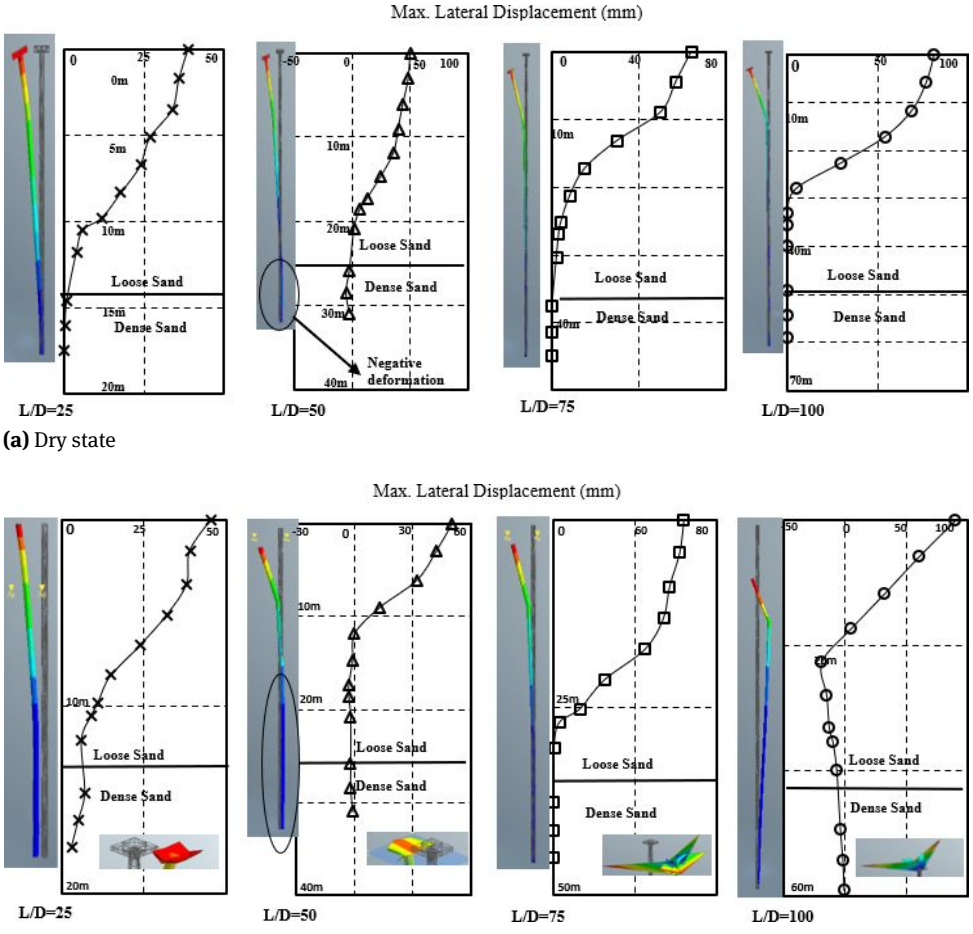

(a) Dry state

(b) Saturated state

Figure 3: Lateral pile displacement with the depth

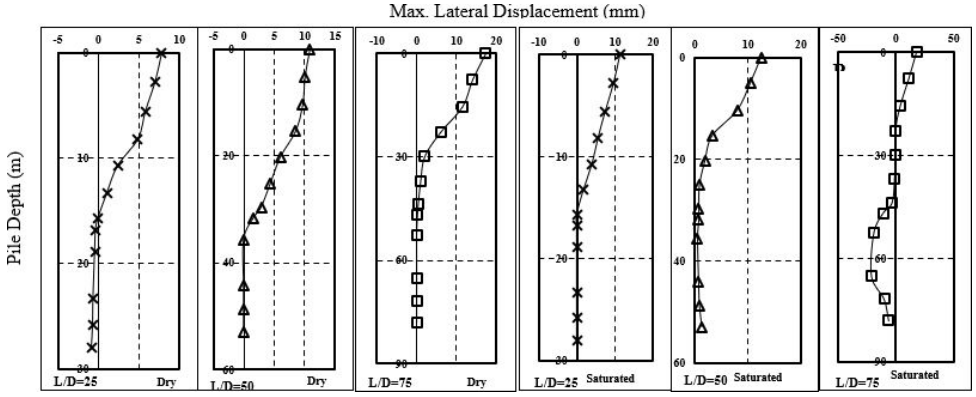

Figure 4: Lateral pile displacement with the depth (D_{pile} = 1 m)

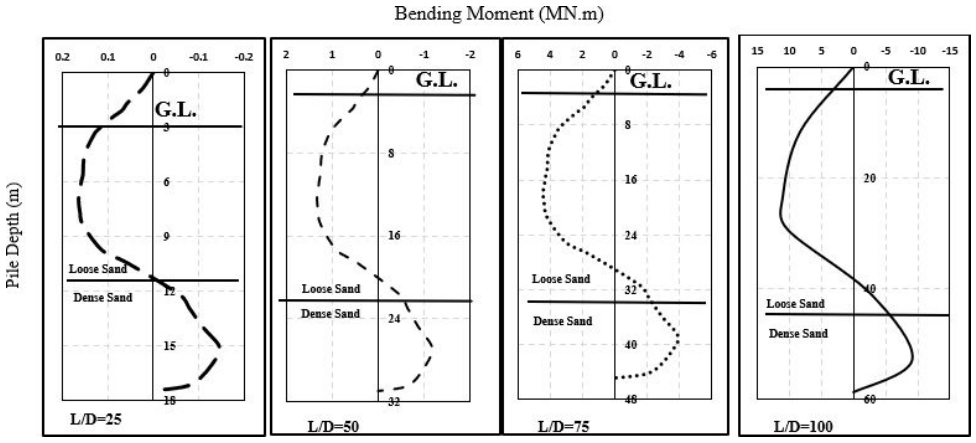

(a) Dry state

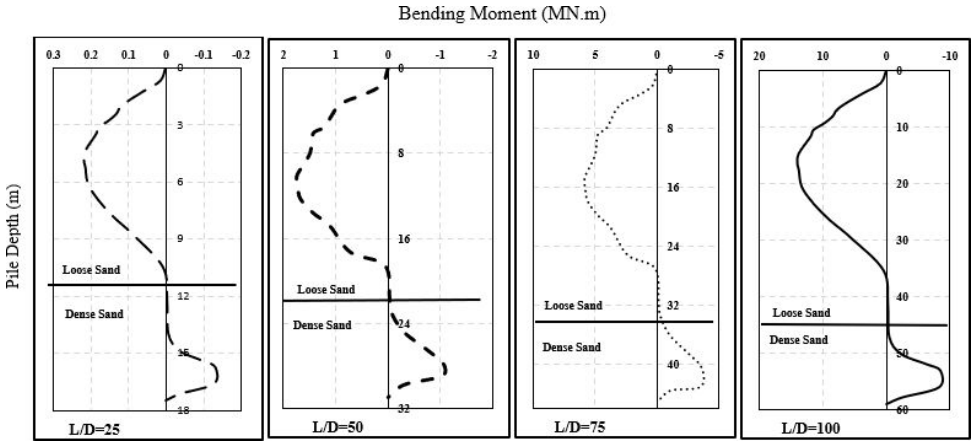

(b) Saturated state

Figure 5: Maximum bending moment along the pile shaft at the PGA on the pile head (around 8.63 seconds)

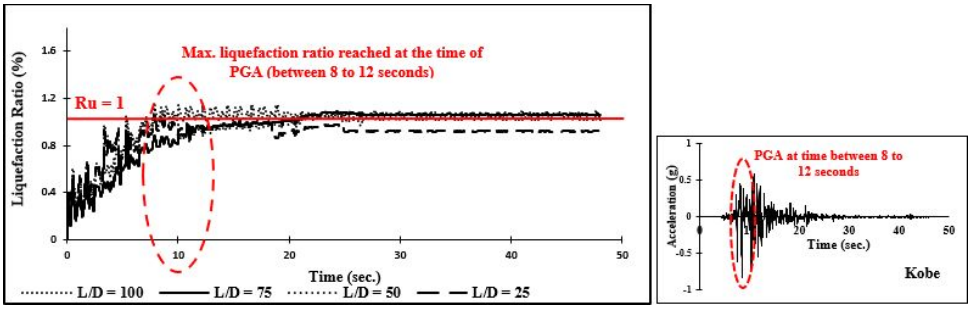

Figure 6: The liquefaction and acceleration time history

settlements developed from the ground shaking. Once the excess pore water pressure reaches the initial vertical effective stress of the selected soil, the shear strength of the soil decreases and then. Figure 6 depicts the propagation of the excess pore water pressure ratio over time with different slenderness ratios (L/D = 25, 50, 75, and 100). The liquefaction ratio reached the peak value at a zone below the soil surface and closed to the pile shaft (about 100%) in time between 10 to 20 seconds as the earthquake starts. It is important to mention that no liquefaction developed around the pile tip, since the peak value was about 23% and the soil softening did not develop.

Pile frictional resistance was estimated based on the stresses on the soil-pile interface elements. It is observed that the frictional resistance diminishes during dynamic excitation; specifically, when the pile is embedded in satu-

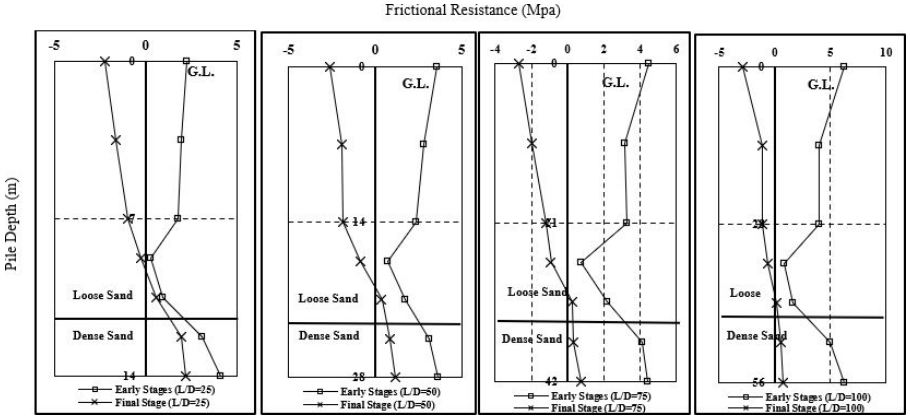

(a) Dry condition

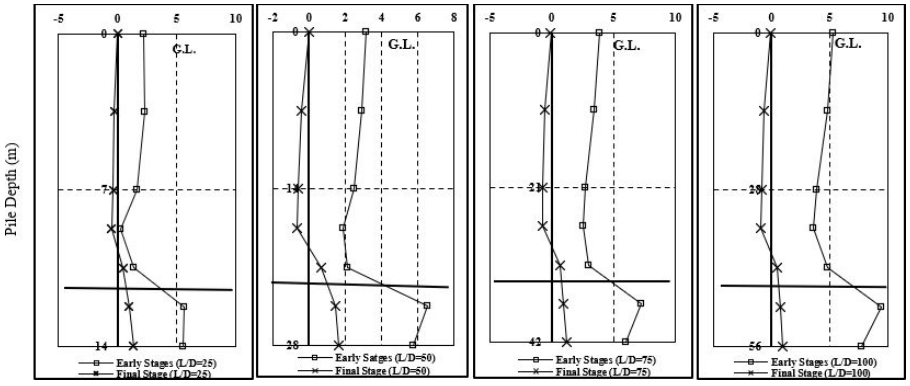

(b) Saturated condition

Figure 7: Frictional resistance of the pile shaft

rated soil layers. The latter may be attributed to the liquefaction phenomenon which in turn significantly decreases the soil shear strength. Similar observations was noticed by Fattah *et al.* [22]. Figure 7 shows Numerical analyses of frictional resistance along the pile length embedded in saturated soil.

4 Conclusions

In this research, the soil-pile interaction behavior was investigated using 3D finite element concepts under the influence of combined static-dynamic loads. The applicability of using MIDAS GTS NX with two constitutive models (modified Mohr-Coulomb and modified UBCSAND) to estimate the onset of liquefaction and the post-liquefaction response was demonstrated. An aluminum pile was embedded in dry and saturated sand soil (Karbala'a soil) where the tests were performed in the laboratory. The soil parameters for modified Mohr-Coulomb and modified UBCSAND models were obtained from simple laboratory tests and then calibrated based on published correlations. To restrict the wave reflection of the lateral reaction and interference of the model based on the vertical reaction, free field elements were generated around model sides (in the direction of applied ground motion) and elastic boundary conditions were employed at the bottom of the model, respectively. Consequently, four different slenderness ratios (25, 50, 75, and 100) were used with two different soil conditions (dry and saturated). The main results of L/D = 25 were validated with the experimental works of the shaking table test [19, 20]. The current paper presents the following conclusions:

- Once the passive resistance at the head and tip is reached, failure happens at the tip. In the situation of a long pile, in which it is observed that the overall net passive resistance created at the lowest portion of the pile is rather high (as shown in Figure 7), and so a pile can not move (as shown in Figure 3).
- In the dry condition at a slenderness ratio of 25, the pile lateral resistance is roughly linear within the loose sand layer. Then, the pile experiences nonlinear relationship at higher slenderness ratio which

is more than 25 (Figure 3(a)), revealing that the failure happened in the pile and it is now acting like a flexible pile. In general, the pile lateral displacements with all conditions were too high and exceeded the maximum tolerable value due to the small pile diameter (0.56 m) with respect to the slenderness ratios (25, 50, 75, 100) which in turn affect the pile stiffness. Additionally, the intensity of the Kobe acceleration is extremely high (PGA about 0.82g). However, the lateral displacements were roughly reasonable when the diameter of the pile increased to 1m with the slenderness ratios of 25 and 50 under similar circumstances.

- To obtain stability to resist moments caused by horizontal stresses, a pile must be sufficiently embedded in the non-liquefiable soil layer beneath the liquefiable one. The pile may move because of kinematic stresses if sufficient fixity is not obtained.
- A pile experienced remarkable deformation due to a significant reduction in soil stiffness when the adjacent loose sand soil experienced liquefaction (excess pore water pressure ratio >85%).

Acknowledgement: The authors would like to thank Dr. Rusal Hussien, for providing the laboratory experimental results used to validate the numerical outputs in this paper.

Funding information: The authors state no funding involved.

Author contributions: All authors have accepted responsibility for the entire content of this manuscript and approved its submission.

Conflict of interest: The authors state no conflict of interest.

References

[1] Davis EH, Poulos HG. Pile Foundation Analysis and Design. New York: Wiley; 1980. Available https://catalogue.nla.gov.au/Record/2877390.

[2] Al-Salakh AM, Albusoda BS. Experimental and Theoretical Determination of Settlement of Shallow Footing on Liquefiable Soil. J Eng. 2020;26(9).

[3] Muqtadir A, Desai CS. Three-Dimensional Analysis of Pile-Group Foundation. Int J Numer Anal Methods Geomech. 1986;10(1):41–58.

[4] Karthigeyan S, Ramakrishna VG, Rajagopal K. Numerical investigation of the effect of vertical load on the lateral response of piles. J Geotechn Geoenviron Eng. 2007;133(5):512–521.

[5] Al Ghanim AA, Mohammed Shafiqu QS, Ibraheem AT; AL-Ghanim AR. Shafiqu QSM, Ibraheem AT. Finite Element Analysis of the Geogrid-Pile Foundation System under Earthquake Loading. Al-Nahrain J Eng Sci. 2019;22(3):202–7.

[6] Almashhadany OY, Albusoda BS. Effect of Allowable Vertical Load and Length/Diameter Ratio (L/D) on Behavior of Pile Group Subjected to Torsion. J Eng. 2014;20(12).

[7] Sitharam TG. Advanced Foundation Engineering. 1^{st} ed. Boca Raton: CRC Press; 2019.

[8] Jie Han. Laterally Loaded Single Piles. Lecture Note of Advanced Foundation Engineering. The University of Kansas; 2015.

[9] Fleming K, Weltman A, Randolph M, Elson K. Piling Engineering. 3rd ed. New York: Routledge Taylor & Francis; 2009.

[10] Bhattacharya S, Tokimatsu K. Essential criteria for design of piled foundations in liquefiable soils. 39^{th} Japan National Conference on Geotechnical Engineering; 2004 Jul 7-9; Niigata, Japan. 2004. p. 1805–1806.

[11] Bhattacharya S, Bolton M. Buckling of piles during earthquake liquefaction. Proceedings of 13th World Conference on Earthquake Engineering; 2004 Aug 1-6; Vancouver, Canada. 2004. p 1-4.

[12] Eurocode 8: Design Provisions for Earthquake Resistance of Structures. London: British Standards Institution; 1996.

[13] NEHRP. NEHRP Recommended provisions for seismic regulations for new buildings and other structures. Part 1 Provisions, FEMA 368. Washington (D. C.): Federal Emergency Management Agency; 2000.

[14] Temperoni B, Viñas MB, Diovisalvi N, Negri R. Seasonal production of *Oithona nana* Giesbrecht, 1893 (Copepoda: Cyclopoida) in temperate coastal waters off Argentina. J Plankton Res. 2011;33(5):729–40.

[15] Iman A, Saad F, Karim H. Effect of the Slenderness Ratio of Piles on Ultimate Lateral Resistance in Sandy Soil. Eng Technol J. 2021;39(12):1740–7.

[16] Al-Jeznawi D, Jais IB, Albusoda BS. Numerical Evaluation of the Nonlinear Behavior of Soil-Pile Interaction Under the Effect of Coupled Static-Dynamic Loads. Bull Earthquake Eng. To be published 2022a.

[17] Al-Jeznawi D, Jais IB, Albusoda BS. The Effect of Model Scale, Acceleration History, and Soil Condition on Closed-Ended Pipe Pile Response under Coupled Static- Dynamic Loads. Int J Appl Sci Eng. To be published 2022b.

[18] Beaty MH, Byrne PM. UBCSAND Constitutive Model Version 904aR. Documentation Report: UBCSAND Constitutive Model on Itasca UDM Web Site. 2011.

[19] Hussein RS, Albusoda BS. Experimental and Numerical Analysis of Laterally Loaded Pile Subjected to Earthquake Loading. Modern Applications of Geotechnical Engineering and Construction. Singapore: Springer; 2021a. p. 291–303.

[20] Hussein RS, Albusoda BS. Experimental Modelling of Single Pile under Combined Effect of Axially and Laterally Loadings in Liquefiable Soil. Geotech Geol Eng. To be published 2021b.

[21] Robinsky E, Morrison C. Sand displacement and compaction around model friction piles. Can Geotech J. 1964;81(2):93–1.

[22] Fattah MY, Zbar BS, Mustafa FS. Effect of soil saturation on load transfer in a pile excited by pure vertical vibration. Proc Inst Civ Eng, Struct Build. 2021;174(2):132–44.